

**Multiscale Simulations of Lamellar PS-PEO Block Copolymers doped with LiPF₆
Ions: Supplementary Information**

Vaidyanathan Sethuraman,¹ Santosh Mogurampelly,¹ and Venkat Ganesan^{1, a)}

*Department of Chemical Engineering, University of Texas at Austin, Austin,
Texas 78712, USA*

^{a)}Electronic mail: venkat@che.utexas.edu.

UNITED ATOM PARAMETERS

Bonding Potential: $V_b = k_b(r - r_0)^2$				
Type	k_b (kcal/mol/(Å) ²)	r_0 (Å)		
CH ₂ -CH ₂	250	1.54		
CH-CH ₂	250	1.54		
CH-CH ₃	250	1.51		
CH(ring)-CH(ring)	250	1.40		
C(ring)-CH(ring)	250	1.40		
C(ring)-CH ₂	250	1.51		
O-CH	250	1.41		
P-F	190	1.6		
Angle Potential: $V_\theta = k_\theta(\theta - \theta_0)^2$				
Type	k_θ (kcal/mol/rad ²)	θ_0 (deg)		
CH ₂ -CH ₂ -CH ₂	120	114		
CH(ring)-CH(ring)-CH(ring)	120	120		
CH-CH ₂ -CH	62	114		
C(ring) - CH(ring)-CH(ring)	120	120		
CH(ring)- C(ring) -CH	120	120		
CH ₂ - C(ring) - CH ₂	120	120		
CH ₂ -O -CH ₂	60	114		
CH ₂ -CH ₂ - O	50	112		
Dihedral Potential: $V_\phi = \sum_{i=1}^4 \frac{1}{2}k_{i\phi} (1 + (-1)^{(i+1)}) \cos(i\phi)$				
Type	$k_{1\phi}$ (kcal/mol)	$k_{2\phi}$	$k_{3\phi}$	$k_{4\phi}$
O-CH ₂ -CH ₂ -CH ₂	0.7020	-0.2120	0.30600	0
CH ₂ -CH ₂ -O-CH ₂	2.8828	-0.6508	2.2184	0
CH ₂ -CH ₂ -O-CH ₃	2.8828	-0.6508	2.2184	0

CH ₂ -C(ring) -CH ₂ -C(ring)	1.4112	-0.2712	3.1452	0
CH ₃ -C(ring) -CH ₂ -C(ring)	1.4112	-0.2712	3.1452	0
Non-bonded Potential: $V_{ij} = 4\epsilon_{ij} \left[\left(\frac{\sigma_{ij}}{r_{ij}} \right)^{12} - \left(\frac{\sigma_{ij}}{r_{ij}} \right)^6 \right] + \frac{q_i q_j}{r_{ij}}$; $\epsilon_{ij} = \sqrt{\epsilon_i \epsilon_j}$; $\sigma_{ij} = \frac{\sigma_i + \sigma_j}{2}$				
Type	ϵ (kcal/mol)	σ (Å)	q (e)	
C(ring)	0.0596	3.700	0.0	
CH(ring)	0.1003	3.695	0.0	
CH	0.0199	4.650	0.0	
CH ₂ (PS)	0.0914	3.950	0.0	
CH ₃	0.1947	3.750	0.0	
CH ₂ (PEO)	0.0914	3.950	0.25	
O	0.1093	2.800	-0.5	
Li	0.4000	1.400	1.0	
P	0.2000	3.742	0.7562	
F	0.0610	3.118	-0.2927	

TABLE S1: Interaction parameters for PS-PEO united atom model.

SCMF COARSE-GRAINED POTENTIAL PARAMETERS

Bonding Parameters	
Type	r_0/b
A-A	1.0
A-B	0.872
B-B	1.242
Angle Potential: $V_\theta = k_{\theta, cg} (\cos(\theta) - \cos(\theta_0))^2$	

Type	k_{cg}	θ_0 (degrees)
AAA	2.06	109
AAB	1.989	109
ABB	1.989	130
BBB	1.528	109

TABLE S2: Interaction parameters for PS-PEO coarse-grained SCMF model.

I. COMPUTATION OF RDF IN PS AND PEO DOMAINS

For computing the RDF in the individual domain, the volume of the bin was calculated separately for each reference atom, since periodic boundary conditions are not imposed in the z -direction. The elemental “ideal” volume of the spherical cap ($dV(r)$) at a distance r from each reference atom is then computed using $dV(r) = (2\pi r (r + |z_{int} - z_i|)dr)$, where z_{int} and z_i represent the z coordinates of the nearest interface and the reference particle respectively. We cut-off the RDF at a distance equal to half the domain width.

II. INVERSE COARSE-GRAINING PROCEDURE DETAILS

In this work, we have fitted the histograms in Figures 2(a) and (b) to single Gaussian curve. Such procedure is expected to work for single modal curves. There can be slight error in the case of BBB angles since the distribution is asymmetric. However, we expect that any discrepancies between the coarse-grained potential vs atomistics configurations will not prove significant due to the period of equilibration at the atomistic level, which is enforced in the third stage of our strategy (see main text).

INITIAL AND FINAL CONFIGURATION OF IONS

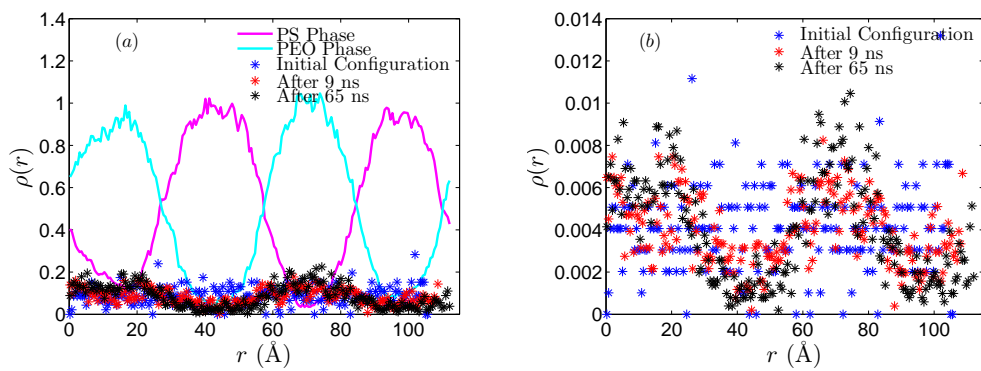


FIG. S1. Evolution of density profiles of (a) Lithium ions along with the initial density profile for PS and PEO; (b) Only Lithium ions

LI-EO COORDINATION IN PEO HOMOPOLYMER MELTS: EFFECTS OF SALT CONCENTRATION

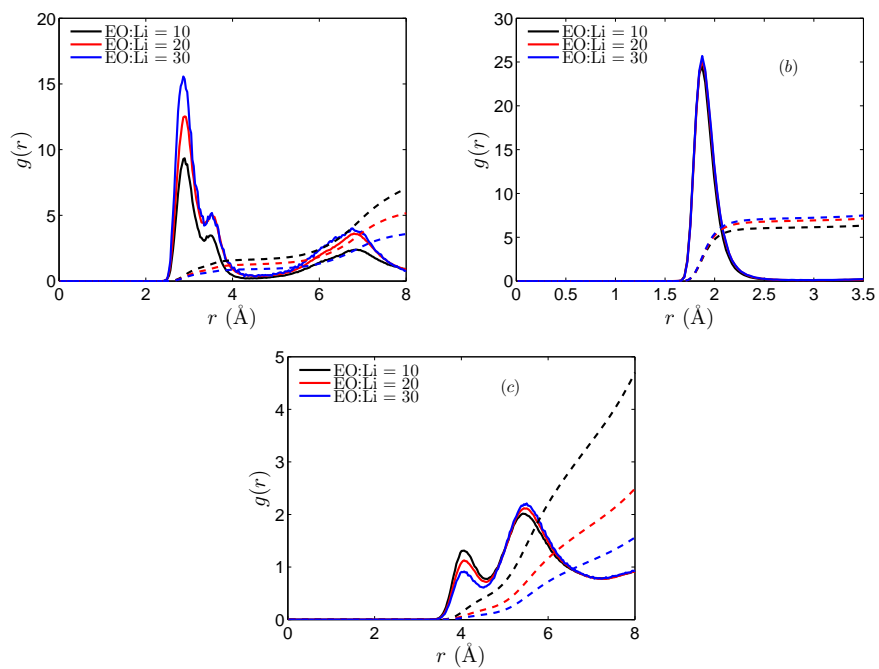


FIG. S2. Homopolymer $g(r)$ and $n(r)$. (a) Li-PF₆; (b) Li-O; and (c) P-O

III. CLUSTER ANALYSIS

An alternate characterization of aggregates were also effected through a “cluster” analysis meant to identify connected structures. For this purpose, we effected a cluster analysis using the methodology proposed by Sevick *et.al.*,¹ in which the ion pair clusters were identified through a connectivity matrix. The cut-off criteria between ion-pairs was again chosen as $r_c = 4.5 \text{ \AA}$. Sequences Li-PF₆-Li-PF₆... and PF₆-Li-PF₆-Li... were considered as part of the same kind of clusters. Subsequently, we computed the average fractions of particles in a cluster of size s as;

$$H_s = \frac{sC_t(s)}{C_p} \tag{1}$$

where $C_t(s)$ and C_p represent the average number of Li-PF₆ clusters of size s and the total number of ion-pairs respectively.

We note that the quantity measured using $H(s)$ is different from Li-PF₆ aggregates or $N(s)$ as defined in Part 2 of Section 2.2.2 of main text, since $H(s)$ computes an ion-cluster (quantifying the overall aggregation) where as $N(s)$ computes the average PF₆ neighbors per Li ions (quantifying the aggregates in the first shell). To distinguish, $N(s)$ is referred to as Li-PF₆ “aggregates”, whereas $H(s)$ is referred to as Li-P “clusters”.

Figure S3 displays the Li-PF₆ cluster size distributions for the different salt concentrations. At the lowest salt concentration, clusters are seen to be limited to sizes less than 5 units. At larger salt concentrations, bigger clusters of the order of 10 pairs are seen to be formed in the system. However, in all cases, Li-PF₆ pair are seen to dominate the distribution. Further, at very low salt concentrations, fraction of single Li-PF₆ cluster (not shown here) dominates far more than other type of clusters. Such results can be rationalized as a direct consequence of the lower density of the system (cf. Table 1) and the smaller number of ions which reduces the number of larger aggregates. Further, the density of the system increases with increasing salt concentration. At the largest salt concentration investigated (EO:Li=10:1), there is a larger propensity to aggregate into larger clusters owing to the crowding of ions inside the system. Such trends are reflected in the higher fraction of longer clusters (12 – 14 LiPF₆ pairs) for the largest ion concentration. At intermediate ion concentration, the density is not significantly

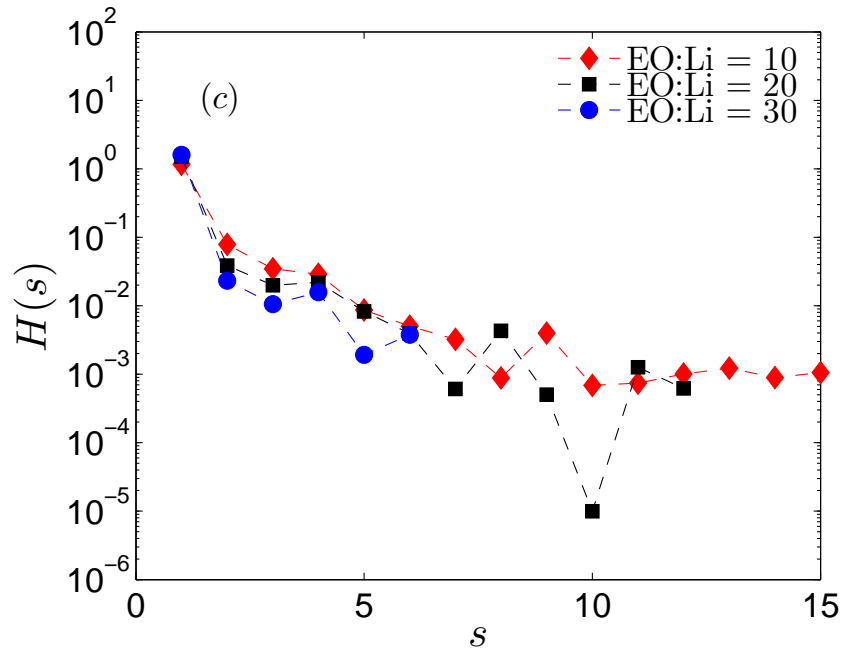


FIG. S3. Number of clusters normalized by the total number of clusters in the system for EO:Li = 20:1.

larger and there does not exist sufficient ions to form larger clusters, and hence the fraction of smaller clusters (2-8) is found to be large, whereas the number of longer clusters (≥ 10) is found to be small.

REFERENCES

¹E. M. Sevick, P. A. Monson, and J. M. Ottino, *The Journal of Chemical Physics* **88**, 1198 (1988).